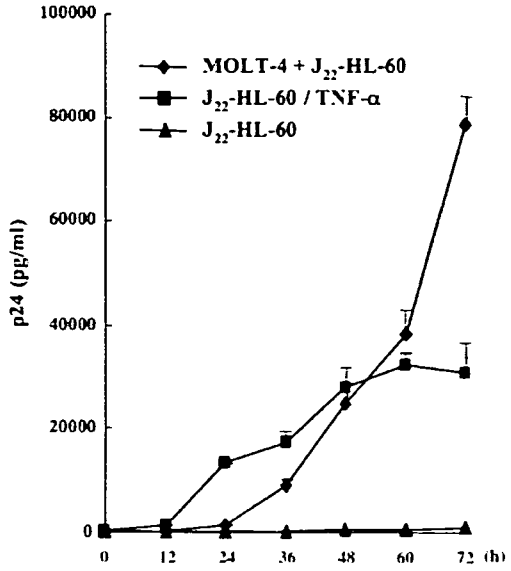

Fig. 2. Kinetics of HIV-1 replication in J_{22}-HL-60 cells. J_{22}-HL-60 cells (2×10^5 cells/ml) were co-cultured with MOLT-4 cells (2×10^5 cells/ml) or treated with TNF-α (1 ng/ml) for the indicated time periods. The p24 antigen released in the culture supernatant was quantified with Lumipulse. Results shown are means±SD from three independent experiments done in duplicate.

Co-culture-induced p24 release does not depend on TNF-α

Because some cytokines are known to induce HIV-1 replication, we investigated by RT-PCR how co-culture of J_{22}-HL-60 and MOLT-4 cells influences mRNA expression of cytokines. Total RNA was isolated 24 and 48 h after co-culture and subjected to quantitative RT-PCR or semi-quantitative RT-PCR analysis. The results of quantitative RT-PCR clearly demonstrated that expression of mRNAs for IL-1β, TNF-α or M-CSF was significantly up-regulated in the mixture of the two types of cells at 24 and 48 h, when compared to MOLT-4 or J_{22}-HL-60 cells cultured independently (Fig. 4A). Semi-quantitative PCR studies revealed that levels of mRNAs for other cytokines including IL-2, IL-4, IL-8, IL-10, IFN-γ, and GM-CSF remained unchanged after co-culture (data not shown). Based on these results, we next tested recombinant cytokines TNF-α, IL-1β and M-CSF for induction of HIV-1 replication in J_{22}-HL-60 cells. Among these, only TNF-α was able to induce release of p24 in J_{22}-HL-60 cells. To determine if TNF-α plays a role in the co-culture-induced HIV-1 replication, J_{22}-HL-60 and MOLT-4 cells were treated with either anti-TNF-α antibody or control mouse IgG for 3 h before and during co-culture. As expected, anti-TNF-α antibody markedly suppressed TNF-α-mediated induction of p24 release from J_{22}-HL-60 cells. However, the co-culture-induced p24 release was virtually unaffected in the presence of anti-TNF-α antibody (Fig. 4B).

NF-κB mediates co-culture-induced p24 release

To investigate if NF-κB is involved in the co-culture-induced p24 release, we first analyzed the phosphorylation status of IκBα by Western blotting because phosphorylation of IκBα usually precedes NF-κB activation induced by extracellular stimuli such as TNF-α and LPS. Phosphorylation of IκBα at the Serine 32 residue was induced in a relatively slow kinetics with a peak at 60 to 120 min after starting co-culture of J_{22}-HL-60 and MOLT-4 cells (Fig. 5A, right panel), whereas TNF-α stimulation led to a rapid phosphorylation of IκBα as early as 5 min after stimulation. This phosphorylation decreased at 60 min and then increased again (Fig. 5A, left panel). Consistently, TNF-α stimulation resulted in a nearly complete disappearance of IκBα within 30 min, while co-culture induced a moderate decrease in IκBα 1 to 2 h later (Fig. 5A).

To further characterize the status of NF-κB activation, we examined NF-κB DNA binding activity, using a ^{32}P-labeled

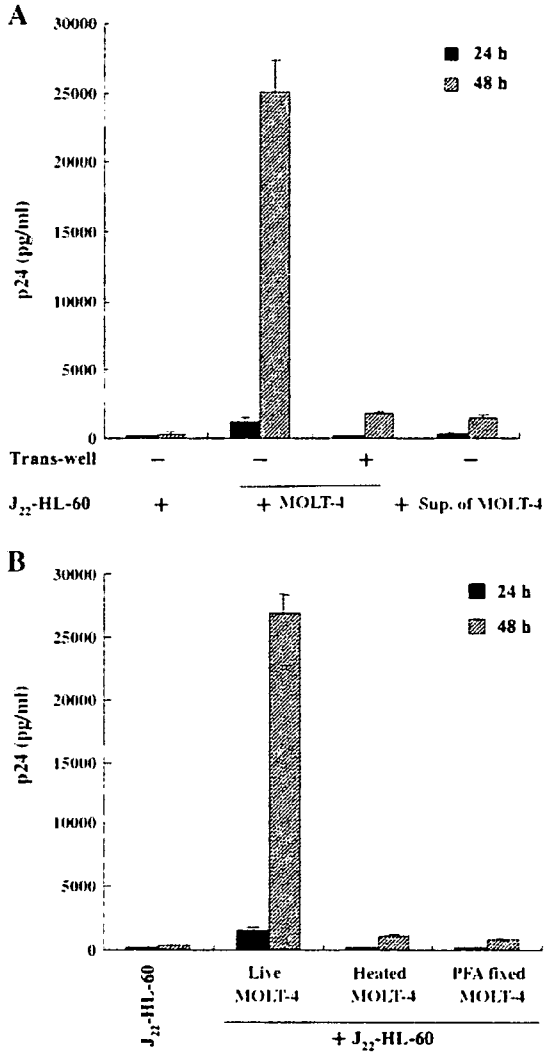

Fig. 3. Live cell contact is required for the co-culture-induced HIV-1 replication. (A) J_{22}-HL-60 cells were either co-cultured with MOLT-4 cells, or seeded separately in trans-well inserts, or treated with the supernatants of MOLT-4 cells. The amount of p24 antigen in the supernatants was measured with Lumipulse at 24 and 48 h. (B) J_{22}-HL-60 cells were co-cultured with either live, heated or paraformaldehyde-fixed MOLT-4 cell for 24 and 48 h. The release of p24 in the culture supernatants was quantified with Lumipulse. Results shown are means±SD from three independent experiments done in duplicate.

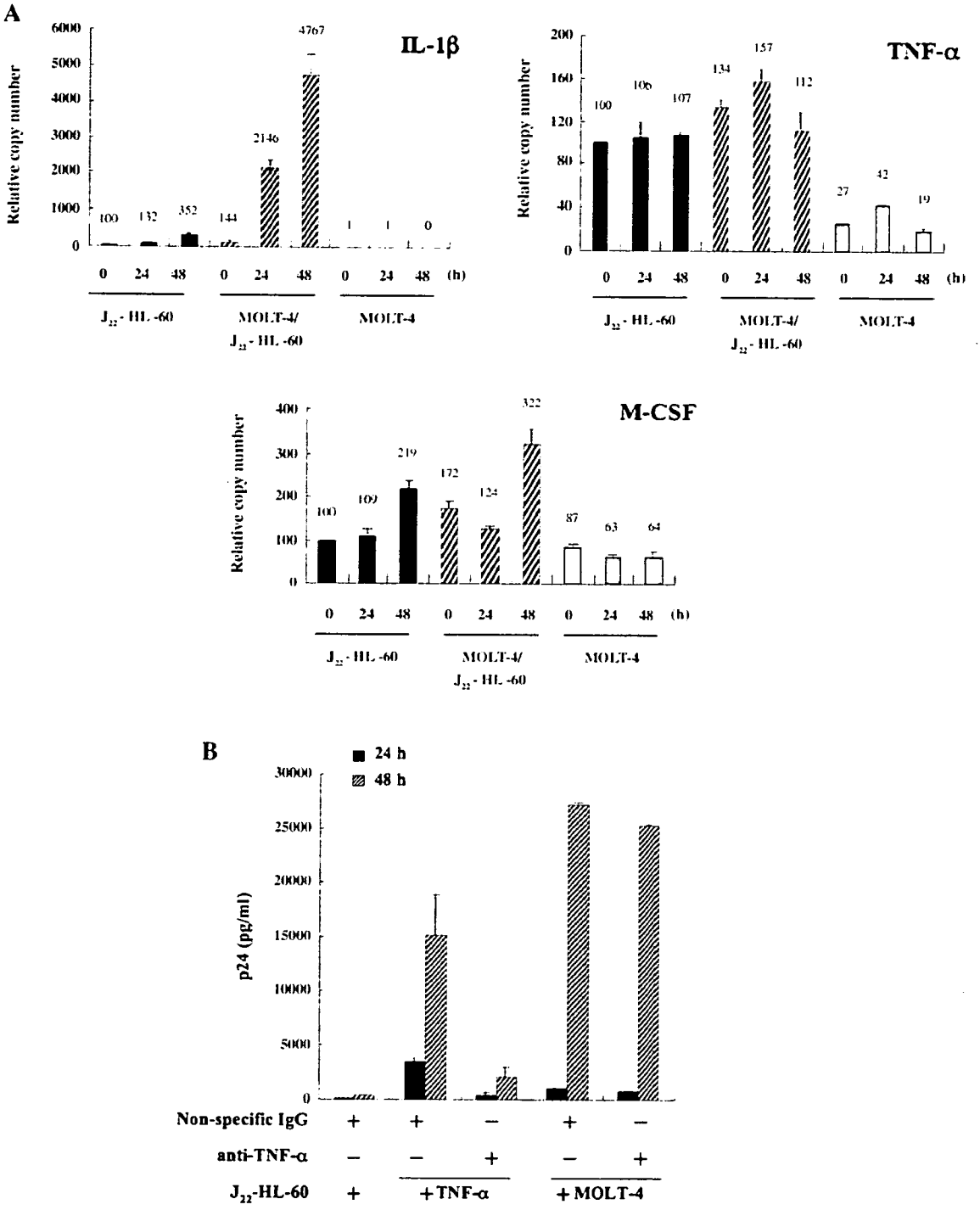

Fig. 4. Induced expression of mRNA for cytokines in co-cultured cells. (A) cDNAs prepared from J_{22}-HL-60 cells alone, MOLT-4 cells alone or co-cultured J_{22}-HL-60 and MOLT-4 cells at 0, 24 or 48 h were subjected to quantitative PCR and the amount of target transcripts was normalized by 18S ribosomal RNA. The copy number of each cytokine in J_{22}-HL-60 cells at 0 h was taken as 100 and relative copy numbers at the indicated time points are shown. (B) J_{22}-HL-60 and MOLT-4 cells were treated with 1500 ng/ml of anti-TNF-α antibody at 37 °C for 2 h before and during co-culture. Released p24 in the culture supernatants was quantified with Lumipulse. Data shown are means±SD from three independent experiments done in duplicate. Isotype-matched nonspecific antibodies were used in control experiments.

synthetic oligonucleotide containing the HIV-1 κB tandem motif. The results showed that the NF-κB DNA binding activity reached a peak around 2 h after starting co-culture (Fig. 5B). To know if NF-κB plays a key role in co-culture-mediated HIV-1 replication, J_{22}-HL-60 cells were infected with retrovirus capable of expressing a super-repressor form of IκBα (SR-IκBα) that can specifically suppress NF-κB-dependent transcription (Brockman et al., 1995). The viability of J_{22}-HL-60

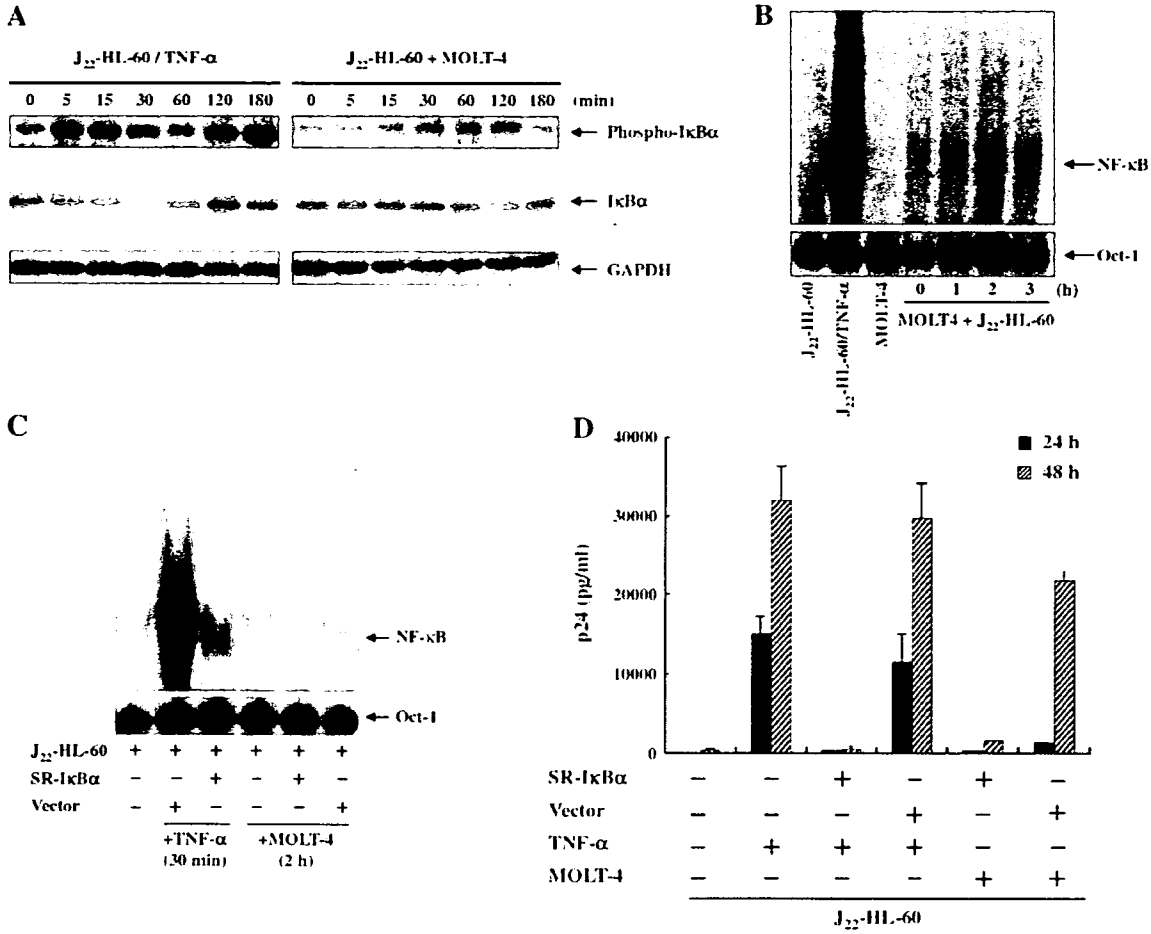

Fig. 5. NF-κB mediates co-culture-induced p24 release. (A) Whole cell lysates (30 μg/lane) prepared from J_{22}-HL-60 cells stimulated with TNF-α or co-cultured with MOLT-4 cells for the indicated time periods were separated on a 10% polyacrylamide gel and subjected to Western blotting with anti-phospho-IκBα, anti-IκBα or anti-GAPDH antibodies. (B) Nuclear extracts prepared from J_{22}-HL-60 cells, J_{22}-HL-60 cells stimulated with 1 ng/ml of TNF-α for 30 min, MOLT-4 cells or co-cultured J_{22}-HL-60 and MOLT-4 cells were subjected to electrophoretic mobility shift assay with a ^{32}P-labeled κB DNA probe. Oct-1 binding was studied in parallel to verify equivalent loading. (C) J_{22}-HL-60 cells stably expressing a super-repressor-IκBα (SR-IκBα) or empty vector were stimulated with TNF-α (1 ng/ml) for 30 min or co-cultured with MOLT-4 cells for 2 h. Nuclear extracts were subjected to EMSA as described in panel B. (D) HIV-1 replication was monitored in J_{22}-HL-60 cells stably expressing or not SR-IκBα and either stimulated with TNF-α or co-cultured with MOLT-4 cells. Release of p24 was analyzed at 24 and 48 h later.

cells was not altered by introduction of SR-IκBα (date not shown). Infected J_{22}-HL-60 cells were then stimulated with TNF-α or co-cultured with MOLT-4 cells (Fig. 5C). J_{22}-HL-60 cells expressing SR-IκBα failed to form a significant NF-κB-specific DNA-binding complex in either case. Importantly, expression of SR-IκBα potently suppressed HIV-1 replication in J_{22}-HL-60 cells either stimulated with TNF-α or co-cultured with MOLT-4 cells (Fig. 5D). These results indicated that co-culture activated NF-κB in a unique kinetics, which then played an essential role in co-culture-induced HIV-1 replication in J_{22}-HL-60 cells.

Ritonavir blocks co-culture-induced p24 release through inhibition of NF-κB activation

A previous study suggested that protease inhibitor (PI) pretreatment blocks activation of NF-κB induced by TNF-α or Toll-like receptor ligands (Equils et al., 2004). We examined if ritonavir blocks NF-κB activation induced by cell–cell contact. Treatment with ritonavir for 2 h before and during co-culture efficiently suppressed activation of NF-κB in a dose-dependent manner (Fig. 6A). HIV-1 replication induced by co-culture was almost completely inhibited by 1 μM of ritonavir (Fig. 6B). Based on the SR-IκB results, it is reasonable to assume that pretreatment with ritonavir ablated HIV-1 replication in co-cultured J_{22}-HL-60 cells through NF-κB inhibition.

$CD4^+$ T cells stimulates HIV-1 replication in J_{22}-HL-60 cells

Finally, we asked if primary $CD4^+$ T cells were able to stimulate HIV-1 replication in J_{22}-HL-60 cells. Co-culture with primary $CD4^+$ T cells indeed induced p24 release from J_{22}-HL-60 cells, which was greatly enhanced when primary $CD4^+$ T cells had been stimulated with PHA before co-culture. Again, ritonavir treatment ablated the induced replication of HIV-1 (Fig. 7A). In parallel, we monitored the evolution of expression of

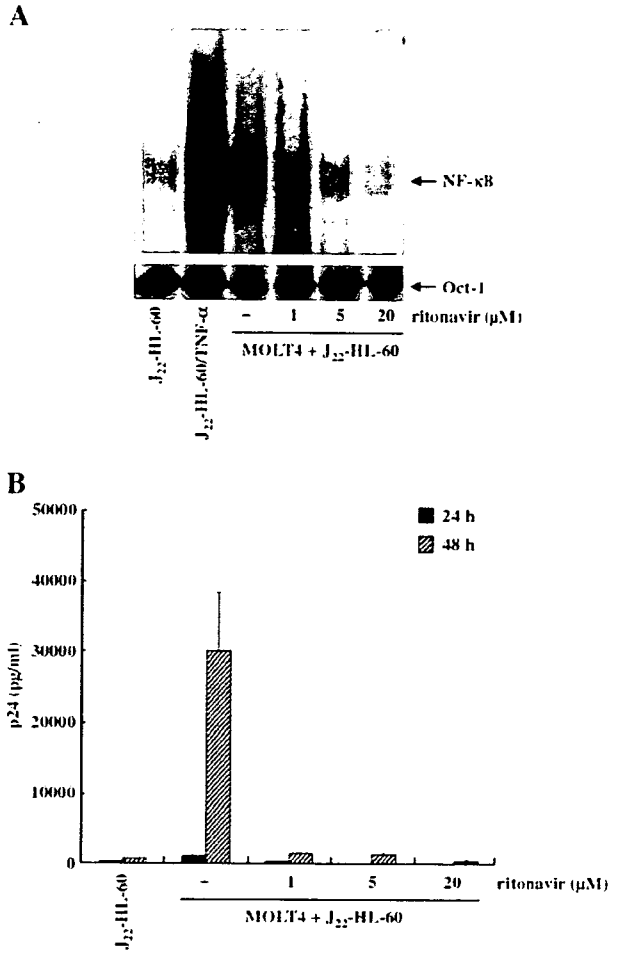

Fig. 6. Ritonavir blocks co-culture-induced p24 release through inhibition of NF-κB activating. (A) Co-cultivation of J_{22}-HL-60 and MOLT-4 cells treated with the indicated concentrations of ritonavir for 2 h was evaluated for NF-κB activation. J_{22}-HL-60 cells stimulated with TNF-α (1 ng/mL) for 30 min were used as a positive control. Oct-1 binding was studied in parallel to verify equivalent loading. (B) J_{22}-HL-60 and MOLT-4 cells treated with ritonavir were subjected to co-culture at a ratio of 1:1. The amount of p24 antigen in supernatants was measured at 24 and 48 h after co-culture.

activation markers in primary $CD4^+$ T cells after co-culture with J_{22}-HL-60 cells pretreated or not with ritonavir. Co-culture with J_{22}-HL-60 cells increased cell surface expression of activation markers CD25 and CD69 in a time-dependent manner, and this activation was not affected by ritonavir (Fig. 7B).

Discussion

We have demonstrated in this study that cell–cell contact is essential for the co-culture-induced HIV-1 replication in J_{22}-HL-60 cells. A variety of membrane proteins including T-cell receptor (TCR) and major histocompatibility complex (MHC) molecules are involved in multiple immune responses. It has been shown that they complete their specific function accompanied with dynamic lateral and vertical movements on the cell membrane during the period of cell-to-cell interaction (Baba et al., 2001). Previous studies have shown that two distinct signals are required for the induction of cell proliferation and cytokine production in resting T cells (Chambers and Allison, 1999; Linsley and Ledbetter, 1993). The first signal is mediated through an interaction between peptide-loaded MHC-II molecules located on APC and the TCR/CD3 complex located on $CD4^+$ T lymphocytes and the second signal is initiated through an interaction between either CD80 or CD86 on the APC and CD28 on $CD4^+$ T cells. In order to investigate whether these two signals are required for the induction of HIV-1 replication in J_{22}-HL-60 cells by cell–cell contact, we analyzed the expression of MHC-II molecules on J_{22}-HL-60 cells (for first signal), CD80 or CD86 on J_{22}-HL-60 cells and CD28 on MOLT-4 cells (for second signal) by FACS analysis. Our results indicated that J_{22}-HL-60 cells express CD80 and CD86 but not MHC-II molecules, and MOLT-4 cells does not express CD28 (unpublished data). Therefore, these two kinds of signal may not be involved in the case of co-cultivation of J_{22}-HL-60 cells and MOLT-4 cells.

Stimulation of a member of the tumor necrosis factor receptor (TNFR) superfamily, including TNFRI (CD120a), TNFRII (CD120b), Fas (CD95), CD40, CD30, CD27, 4-1BB (CD137) and OX40 (CD134), by their ligand molecule has been shown to trigger a variety of cellular activities, such as cell growth, differentiation, immunological responses and programmed cell death (Gruss and Dower, 1995; Chougnet et al., 2001; Herbein, 1997). In particular, TNF superfamily proteins have been reported to enhance HIV-1 replication in cells latently infected with HIV-1; TNF-α has been shown to enhance HIV-1

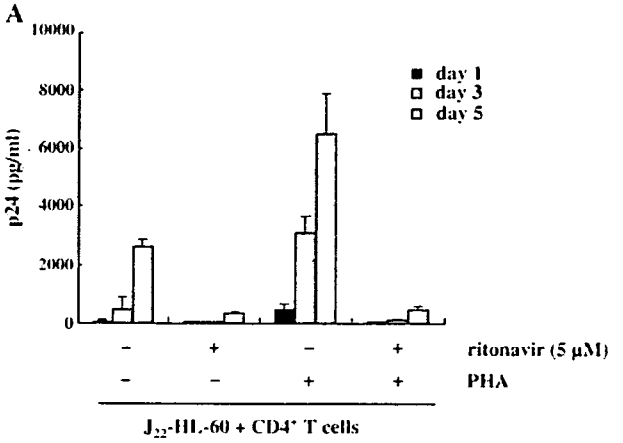

Fig. 7. Activated primary $CD4^+$ T cells efficiently stimulate HIV-1 replication in J_{22}-HL-60 cells. (A) J_{22}-HL-60 cells (2×10^5) were co-cultured with resting or PHA-activated primary $CD4^+$ T cells (1×10^6), which had been isolated from PBMC by a negative selection, with or without ritonavir. The culture supernatants were collected at day 1, day 3 and day 5 after starting co-culture and the levels of p24 antigen were determined. (B) Resting or PHA-activated primary $CD4^+$ T cells were co-cultured with J_{22}-HL-60 cells. CD25 and CD69 expression was analyzed by FACS in resting or PHA-activated primary $CD4^+$ T cells after co-culture with J_{22}-HL-60 cells for 0, 1, 3 or 5 days as described in panel A. The different features of FSC and SSC between $CD4^+$ T cells and J_{22}-HL-60 cells are shown in the upper panel. Expression of CD25 and CD69 on $CD4^+$ T cells was monitored as described in Materials and methods. Isotype controls were included in all assays (date not shown). Numbers in the upper right, left and lower right quadrant indicate percentage of single or double-positive cells. Data are representative of two independent experiments.

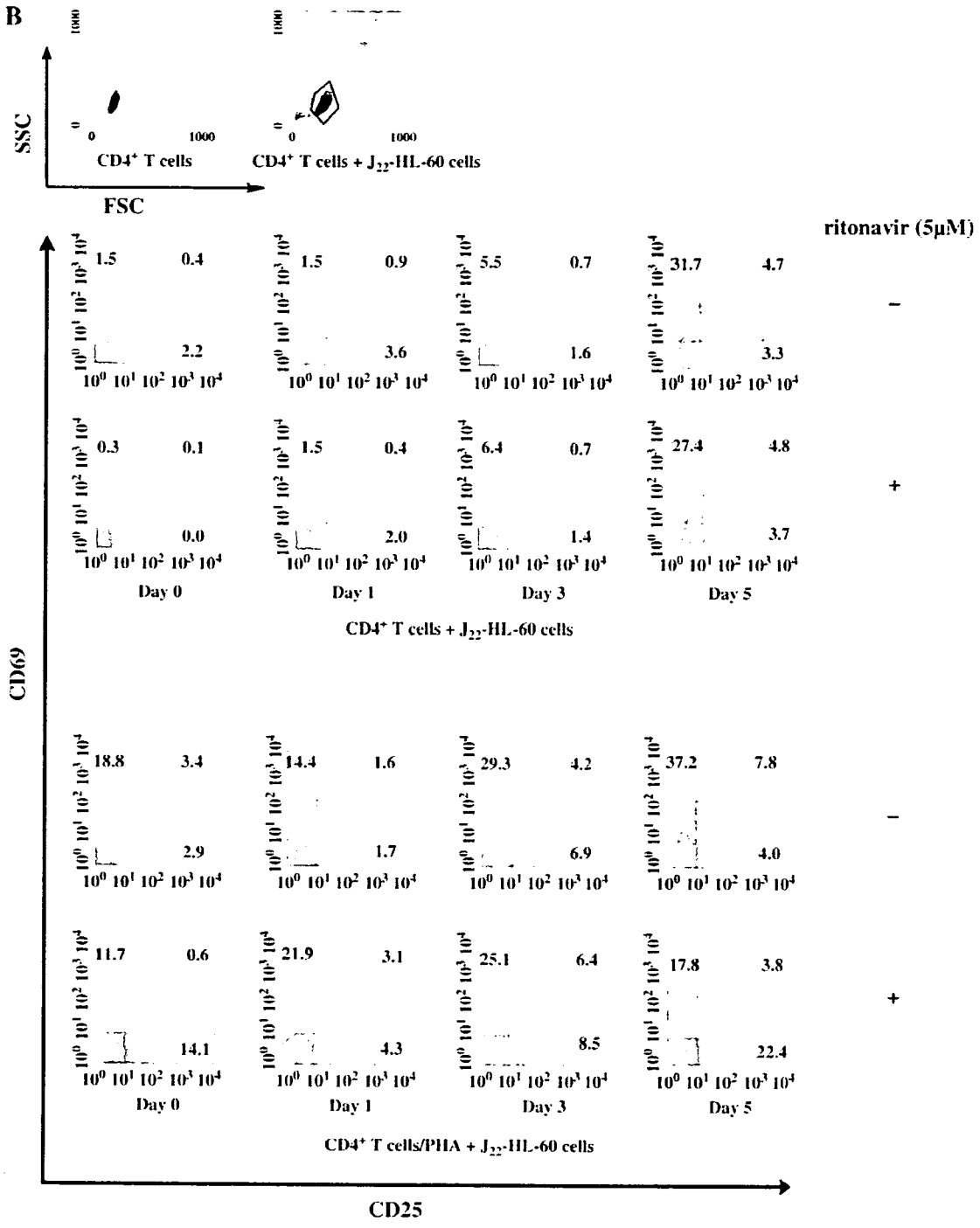

Fig. 7 (*continued*).

replication in mononuclear phagocytes and chronically infected cell lines including J_{22}-HL-60 cells (Matsuyama et al., 1991; Folks et al., 1989; Matsuyama et al., 1989; Osborn et al., 1989); gp34–OX40 interaction through cell–cell contact also induced HIV-1 replication in latently infected T cells (Takahashi et al., 2001). Earlier reports described that up-regulation of cytokine expression by cell–cell contact contributes to replication of HIV-1 in latently infected cells (Devadas et al., 2004; Borghi et al., 2000). In our experiments, although expression of mRNA for cytokines M-CSF, TNF-α and IL-1β was enhanced by cell–cell contact, M-CSF and IL-1β showed no appreciable effect on virus production in J_{22}-HL-60 cells. Moreover, neutralizing antibody against TNF-α was unable to inhibit co-culture-induced HIV-1 replication. Nevertheless, we cannot exclude

possible involvement of cytokines that were not examined in this study, and it is formally possible that such cytokines may be secreted from activated T cells after cell–cell contact and can stimulate J_{22}-HL-60 cells. Paraformaldehyde-fixed MOLT-4 cells failed to induce HIV-1 replication in J_{22}-HL-60 cells. It is thus possible that J_{22}-HL-60 cells somehow stimulated MOLT-4 cells initially, which in turn gave back signals to J_{22}-HL-60 cells and induced HIV-1 replication. This "outside-in" signaling model is consistent with the observed delay in phosphorylation of IκBα, degradation of IκBα and release of p24 induced by cell–cell contact as compared to those induced by TNF-α. The hypothesis was further supported by the evidence that primary $CD4^+$ T cells (both resting and PHA simulated) exhibited elevated levels of surface activation markers CD25 and CD69 by co-culture with J_{22}-HL-60 cells as well as induced the HIV-1 replication of J_{22}-HL-60 cells. Moreover, PHA-simulated primary $CD4^+$ T cells have more efficiency on both enhanced HIV-1 replication and the status of activation of themselves than resting $CD4^+$ T cells (Fig. 7).

The replication of HIV-1 is closely associated with the activation status of its host cells and is dependent on a number of host factors. The HIV-1 long terminal repeat (LTR) contains at least six defined elements that bind cellular transcription factors (Pereira et al., 2000). Among these, the best characterized is NF-κB, which plays important roles in cellular and viral gene expression. In Fig. 5A, TNF-α induced a prominent phosphorylation of IκBα as early as 5 min after stimulation, which subsided by 60 min and then got intensified again. This is consistent with previous reports on the oscillation of IκBα phosphorylation and NF-κB activation following TNF-α stimulation (Hoffmann et al., 2002; Nelson et al., 2004). In contrast, the kinetics of IκBα phosphorylation mediated by co-culture seemed to be slower and more persistent. This may partly explain why co-culture-induced p24 release from J_{22}-HL-60 cells was not remarkable at earlier time points, but finally exceeded that induced by TNF-α. Together with the strong inhibition of p24 release by forced expression of SR-IκBα, which indicates critical involvement of NF-κB activation, the results raise two possibilities as to the mechanism of co-culture-induced HIV-1 replication. First, NF-κB activation in J_{22}-HL-60 cells is necessary, but the kinetics of induction may also be important for HIV-1 replication in J_{22}-HL-60 cells. NF-κB activation by TNF-α is very strong and transient, while that by cell–cell contact may relatively be weak, but rather persistent. Second, signals from T cells that cannot be triggered by TNF-α stimulation may potentiate co-culture-induced sustained HIV-1 replication.

Our recent study demonstrated that an HIV-1 protease inhibitor ritonavir inhibits constitutive NF-κB activation in HUT-102 and primary adult T-cell leukemia cells (Dewan et al., 2006). In this study, we have found that ritonavir not only inhibits the functions of HIV-1 protease, but also suppresses inducible NF-κB activation and down-regulates HIV-1 release from chronically infected cells. This suggests that cessation of an anti-HIV-1 therapy including ritonavir may lead to activated $CD4^+$ T-cell-induced virion production from latently infected cells.

Materials and methods

Cell culture

J_{22}-HL-60 is a monocytic cell line that contains one copy of monocyte-tropic JR-FL HIV-1 strain (Kitano et al., 1990). L428 and KM-H2 are B lymphocytic cell lines. MOLT-4, Jurkat, MT-2 and MT-4 are T-cell lines. All the cell lines used in this study were maintained in RPMI 1640 medium supplemented with 10% fetal bovine serum (FBS) (Cansera International Inc., Canada), 100 μg/ml of penicillin and 100 μg/ml of streptomycin. J_{22}-HL-60 cells (2×10^5/ml) and MOLT-4 cells (2×10^5/ml) were co-cultured in 1.5 ml of the regular medium at ratio of 1:1. For trans-well experiments, J_{22}-HL-60 cells were plated on the plastic substrate of 24-well plates, and MOLT-4 cells were plated in the trans-well insert in the same condition as for co-culture. Supernatants were collected at 24 and 48 h after starting co-culture. Alternatively, J_{22}-HL-60 cells were treated with the supernatant of MOLT-4 cells (2×10^5/ml), which had been filtrated with a 0.45 μm filter and centrifuged at 53,000 rpm for 30 min. $CD4^+$ T cells were isolated from PBMC by negative selection with magnetic beads coated with antibodies that remove non-$CD4^+$ T cells. $CD4^+$ T cells (1×10^6/ml) were washed once with RPMI 1640 medium and co-cultured with J_{22}-HL-60 cells (2×10^5/ml). For activation of $CD4^+$ T cells, $CD4^+$ T cells were pretreated with PHA (5 μg/ml) 1 day before co-culture and washed with RPMI 1640 for 3 times to remove PHA then subjected to co-culture. Supernatants were collected at 24 and 48 h after starting co-culture. Plat-E packaging cells were described previously (Morita et al., 2000) and were maintained in DMEM supplemented with 10% fetal calf serum, blasticidin S (10 μg/ml), puromycin (1 μg/ml), penicillin G (100 U/ml) and streptomycin (100 μg/ml). Plat-E cells were transfected with pMRX-SR-IκBα-puro (pMRX-SR-IκBα-puro was constructed by inserting an *Eco*RI fragment encoding SR-IκBα into the *Eco*RI site of pMRX-puro) or pMRX-puro (Nonaka et al., 2005) using fugene 6 transfection reagent (Roche, Indianapolis, IN, USA). Culture supernatants of Plat-E cells were collected 72 h after transfection and used for infection of J_{22}-HL-60 cells in the presence of 10 μg/ml of polybrene.

Quantification of HIV-1 replication

Culture supernatants were assayed for HIV-1 p24 antigen using an ELISA kit Lumipulse according to the manufacturer's instructions. Assays were performed in triplicate.

Fixation or heat treatment of MOLT-4 cells

MOLT-4 cells were washed three times in 1× PBS (pH 7.2) and incubated either at room temperature for 30 min with 3% paraformaldehyde in 1× PBS or at 60 °C for 10 min. Cells were then washed three times with 1× PBS and twice with RPMI 1640 medium before placing them in co-culture.

Quantitative RT-PCR

Total RNA was extracted using Isogen (Nippon Gene Co., Toyama, Japan), treated with DNase I (GIBCO BRL) and subjected to quantitative RT-PCR. First-strand cDNA synthesis was conducted with 1 μg of total RNA using the SuperScript First-Strand Synthesis System for RT-PCR with random hexamers (Invitrogen Life Technologies, Carlsbad, CA). The amount of target transcripts was subsequently quantified by real-time PCR using ABI 7700 sequence detector system and SYBR green core reagent kit (Applied Biosystems) according to the manufacturer's protocol. The PCR cycling was done with a denaturation step at 95 °C for 10 min and 45 cycles of denaturation (95 °C for 15 s), annealing and extension (60 °C for 3 min). The primer sequences were as follows: for TNF-α, forward: 5′-ACAAGCCTGTAGCCCATGTT-3′ and reverse: 5′-AAAGTAGACCTGCCCAGACT-3′; for IL-1β, forward: 5′-GGATATGGAGCAACAAGTGG-3′ and reverse: 5′-ATGTACCAGTTGGGGAACTG-3′; for M-CSF, forward: 5′-ATGACCGCGCCGGGCGCCGC-3′ and reverse 5′-CTACACTGGCAGTTCCACCT-3′; for 18S ribosomal RNA, forward: 5′-GTAACCCGTTGAACCCCATT-3′ and reverse: 5′-CCATCCAATCGGTAGTAGCG-3′. The copy number of 18S ribosomal RNA normalized the relative copy numbers of target transcripts.

Neutralization with anti-TNF-α antibody

J_{22}-HL-60 cells (2×10^5/ml) and MOLT-4 cells (2×10^5/ml) were treated for 2 h with 1500 μg/ml anti-TNF-α antibody (SIGMA USA) or 1500 μg/ml goat anti-mouse IgG (American Qualex USA) and then placed in co-culture. Supernatants were collected at 24 and 48 h after starting co-culture. Culture supernatants were assayed for HIV p24 antigen production with Lumipulse. Viable cell numbers were determined by trypan-blue dye staining.

Immunoblot analysis

J_{22}-HL-60 cells were co-cultured with MOLT-4 cells or stimulated with TNF-α for 0, 5, 15, 30, 60, 120 or 180 min. Cells were lysed in a lysis buffer (20 mM Tris–HCl [pH 8.0], 150 mM NaCl, 1% Triton X-100, 10% glycerol, 0.5 mM dithiothreitol, 0.5 mM phenylmethylsulfonyl fluoride, 0.1% aprotinin and 0.1% leupeptin), centrifuged at 12,000×*g* for 20 min at 4 °C and mixed with an equal volume of a two-fold concentration sample buffer containing 125 mM Tris–HCl [pH 8.0], 4% sodium dodecyl sulfate (SDS), 20% glycerol, 0.004% bromophenol blue and 2% 2-mercaptoethanol. These samples were boiled for 5 min and then subjected to SDS-polyacrylamide gel electrophoresis (PAGE) on 10% separation gels; they were then electro-blotted onto PVDF membranes (PALL Co., Tokyo, Japan). The membranes were treated overnight with blocking buffer (3% skim-milk in 1× PBS) at 4 °C, washed twice with PBS and incubated with various antibodies diluted with 1% FCS and 0.5% Tween 20 in PBS at room temperature for 1 h. The membranes were washed three times with 0.5% Tween 20 in PBS and incubated with horseradish peroxidase-labeled second antibodies (Amersham International plc., Buckinghamshire, United Kingdom) for 1 h. After a thorough washing, the bound antibodies were visualized with the ECL detection reagent (Amersham) on Hyperfilm-ECL (Amersham).

Preparation of nuclear extracts

Cells were suspended in hypotonic buffer (10 mM HEPES [pH 7.8], 10 mM KCl, 2 mM $MgCl_2$, 1 mM DTT and 0.1 mM EDTA) supplemented with protease and phosphatase inhibitors, 0.1 mM phenylmethylsulfonyl fluoride, 1 μg/ml leupeptin, 1 μg/ml aprotinin, 100 μM Na_3VO_4 and 20 mM β-glycerophosphate. After 10 min incubation at 4 °C, Nonidet P-40 was added to 1%. Soluble and insoluble fractions were separated by centrifugation. The supernatant was recovered as cytoplasmic extract and the nuclear pellet was washed with hypotonic buffer and resuspended in extraction buffer (50 mM HEPES [pH 7.8], 50 mM KCl, 350 mM NaCl, 0.1 mM EDTA, 1 mM DTT, 0.1 mM PMSF, 1 μg/ml leupeptin, 1 μg/ml aprotinin and 2.5% glycerol). After 30 min incubation at 4 °C, with occasional agitation, DNA pellets were eliminated by centrifugation. The supernatant was recovered as a nuclear extract.

Electrophoretic mobility shift assay (EMSA)

Nuclear extracts (5 μg) were incubated in 20 μl of binding buffer (10 mM HEPES [pH 7.8], 100 mM NaCl, 1 mM EDTA, 2.5% glycerol containing 1 μg of poly[d(I–C)] and 0.5 ng ^{32}P-labeled κB probe derived from the H-$2K^b$ promoter (Kieran et al., 1990) or ^{32}P-labeled Oct-1 probe (Mori et al., 2000)) and incubated for 30 min at room temperature. Samples were run on a 5% polyacrylamide gel containing 2.5% glycerol in 0.5× TBE and retarded bands were revealed by autoradiography.

FACS analysis

Activation status of $CD4^+$ T cells was examined with FITC-conjugated anti-CD25 or PE-conjugated anti-CD69 antibodies (DakoCytomation, Carpinteria, CA, USA). The population of $CD4^+$ T cells were gated out by forward and side scatter signals (FSC/SSC) and 20,000 events were processed for each sample at a rate of 300–500 events/s. Dot-plot statistics were calculated by the instrument software (Cell Quest).

Acknowledgments

This work was supported by grants from the Ministry of Education, Science, and Culture; the Ministry of Health, Labor, and Welfare; and Human Health Science of Japan.

References

Andre, P., Groettrup, M., Klenerman, P., de Giuli, R., Booth Jr., B.L., Cerundolo, V., Bonneville, M., Jotereau, F., Zinkernagel, R.M., Lotteau, V., 1998. An inhibitor of HIV-1 protease modulates proteasome activity, antigen presentation, and T cell responses. Proc. Natl. Acad. Sci. U.S.A. 95 (22), 13120–13124.

Baba, E., Takahashi, Y., Lichtenfeld, J., Tanaka, R., Yoshida, A., Sugamura, K., Yamamoto, N., Tanaka, Y., 2001. Functional CD4 T cells after intercellular molecular transfer of 0X40 ligand. J. Immunol. 167 (2), 875–883.

Borghi, M.O., Panzeri, P., Shattock, R., Sozzani, S., Dobrina, A., Meroni, P.L., 2000. Interaction between chronically HIV-infected promonocytic cells and human umbilical vein endothelial cells: role of proinflammatory cytokines and chemokines in viral expression modulation. Clin. Exp. Immunol. 120 (1), 93–100.

Brockman, J.A., Scherer, D.C., McKinsey, T.A., Hall, S.M., Qi, X., Lee, W.Y., Ballard, D.W., 1995. Coupling of a signal response domain in I kappa B alpha to multiple pathways for NF-kappa B activation. Mol. Cell. Biol. 15 (5), 2809–2818.

Bukrinsky, M.I., Stanwick, T.L., Dempsey, M.P., Stevenson, M., 1991. Quiescent T lymphocytes as an inducible virus reservoir in HIV-1 infection. Science 254 (5030), 423–427.

Chambers, C.A., Allison, J.P., 1999. Costimulatory regulation of T cell function. Curr. Opin. Cell Biol. 11 (2), 203–210.

Chougnet, C., Freitag, C., Schito, M., Thomas, E.K., Sher, A., Shearer, G.M., 2001. In vivo CD40–CD154 (CD40 ligand) interaction induces integrated HIV expression by APC in an HIV-1-transgenic mouse model. J. Immunol. 166 (5), 3210–3217.

Collier, A.C., Coombs, R.W., Schoenfeld, D.A., Bassett, R.L., Timpone, J., Baruch, A., Jones, M., Facey, K., Whitacre, C., McAuliffe, V.J., Friedman, H.M., Merigan, T.C., Reichman, R.C., Hooper, C., Corey, L., 1996a. Treatment of human immunodeficiency virus infection with saquinavir, zidovudine, and zalcitabine. N. Engl. J. Med. 334 (16), 1011–1017.

Collier, A.C., Coombs, R.W., Schoenfeld, D.A., Bassett, R., Baruch, A., Corey, L., 1996b. Combination therapy with zidovudine, didanosine and saquinavir. Antivir. Res. 29 (1), 99.

Devadas, K., Hardegen, N.J., Wahl, L.M., Hewlett, I.K., Clouse, K.A., Yamada, K.M., Dhawan, S., 2004. Mechanisms for macrophage-mediated HIV-1 induction. J. Immunol. 173 (11), 6735–6744.

Dewan, M.Z., Uchihara, J.N., Terashima, K., Honda, M., Sata, T., Ito, M., Fujii, N., Uozumi, K., Tsukasaki, K., Tomonaga, M., Kubuki, Y., Okayama, A., Toi, M., Mori, N., Yamamoto, N., 2006. Efficient intervention of growth and infiltration of primary adult T-cell leukemia cells by an HIV protease inhibitor, ritonavir. Blood 107 (2), 716–724.

Duh, E.J., Maury, W.J., Folks, T.M., Fauci, A.S., Rabson, A.B., 1989. Tumor necrosis factor alpha activates human immunodeficiency virus type 1 through induction of nuclear factor binding to the NF-kappa B sites in the long terminal repeat. Proc. Natl. Acad. Sci. U.S.A. 86 (15), 5974–5978.

Equils, O., Shapiro, A., Madak, Z., Liu, C., Lu, D., 2004. Human immunodeficiency virus type 1 protease inhibitors block toll-like receptor 2 (TLR2)- and TLR4-induced NF-kappaB activation. Antimicrob. Agents Chemother. 48 (10), 3905–3911.

Fauci, A.S., 1996. Host factors and the pathogenesis of HIV-induced disease. Nature 384 (6609), 529–534.

Finzi, D., Hermankova, M., Pierson, T., Carruth, L.M., Buck, C., Chaisson, R.E., Quinn, T.C., Chadwick, K., Margolick, J., Brookmeyer, R., Gallant, J., Markowitz, M., Ho, D.D., Richman, D.D., Siliciano, R.F., 1997. Identification of a reservoir for HIV-1 in patients on highly active antiretroviral therapy. Science 278 (5341), 1295–1300.

Folks, T.M., Clouse, K.A., Justement, J., Rabson, A., Duh, E., Kehrl, J.H., Fauci, A.S., 1989. Tumor necrosis factor alpha induces expression of human immunodeficiency virus in a chronically infected T-cell clone. Proc. Natl. Acad. Sci. U.S.A. 86 (7), 2365–2368.

Gruss, H.J., Dower, S.K., 1995. Tumor necrosis factor ligand superfamily: involvement in the pathology of malignant lymphomas. Blood 85 (12), 3378–3404.

Herbein, G., 1997. Cytokines, viruses and macrophages: an interactive network. An immune dysregulation involving the members of the tumor necrosis factor (TNF) receptor superfamily could be critical in AIDS pathogenesis. Pathol. Biol. 45 (2), 115–125.

Hoffmann, A., Levchenko, A., Scott, M.L., Baltimore, D., 2002. The IkappaB–NF-kappaB signaling module: temporal control and selective gene activation. Science 298 (5596), 1241–1245.

Kieran, M., Blank, V., Logeat, F., Vandekerckhove, J., Lottspeich, F., Le Bail, O., Urban, M.B., Kourilsky, P., Baeuerle, P.A., Israel, A., 1990. The DNA binding subunit of NF-kappa B is identical to factor KBF1 and homologous to the rel oncogene product. Cell 62 (5), 1007–1018.

Kitano, K., Baldwin, G.C., Raines, M.A., Golde, D.W., 1990. Differentiating agents facilitate infection of myeloid leukemia cell lines by monocytotropic HIV-1 strains. Blood 76 (10), 1980–1988.

Linsley, P.S., Ledbetter, J.A., 1993. The role of the CD28 receptor during T cell responses to antigen. Annu. Rev. Immunol. 11, 191–212.

Louache, F., Debili, N., Marandin, A., Coulombel, L., Vainchenker, W., 1994. Expression of CD4 by human hematopoietic progenitors. Blood 84 (10), 3344–3355.

Matsuyama, T., Yoshiyama, H., Hamamoto, Y., Yamamoto, N., Soma, G., Mizuno, D., Kobayashi, N., 1989. Enhancement of HIV replication and giant cell formation by tumor necrosis factor. AIDS Res. Hum. Retroviruses 5 (2), 139–146.

Matsuyama, T., Kobayashi, N., Yamamoto, N., 1991. Cytokines and HIV infection: is AIDS a tumor necrosis factor disease? AIDS 5 (12), 1405–1417.

Mori, N., Fujii, M., Iwai, K., Ikeda, S., Yamasaki, Y., Hata, T., Yamada, Y., Tanaka, Y., Tomonaga, M., Yamamoto, N., 2000. Constitutive activation of transcription factor AP-1 in primary adult T-cell leukemia cells. Blood 95 (12), 3915–3921.

Morita, S., Kojima, T., Kitamura, T., 2000. Plat-E: an efficient and stable system for transient packaging of retroviruses. Gene Ther. 7 (12), 1063–1066.

Nelson, D.E., Ihekwaba, A.E., Elliott, M., Johnson, J.R., Gibney, C.A., Foreman, B.E., Nelson, G., See, V., Horton, C.A., Spiller, D.G., Edwards, S.W., McDowell, H.P., Unitt, J.F., Sullivan, E., Grimley, R., Benson, N., Broomhead, D., Kell, D.B., White, M.R., 2004. Oscillations in NF-kappaB signaling control the dynamics of gene expression. Science 306 (5696), 704–708.

Nonaka, M., Horie, R., Itoh, K., Watanabe, T., Yamamoto, N., Yamaoka, S., 2005. Aberrant NF-kappaB2/p52 expression in Hodgkin/Reed-Sternberg cells and CD30-transformed rat fibroblasts. Oncogene 24 (24), 3976–3986.

Osborn, L., Kunkel, S., Nabel, G.J., 1989. Tumor necrosis factor alpha and interleukin 1 stimulate the human immunodeficiency virus enhancer by activation of the nuclear factor kappa B. Proc. Natl. Acad. Sci. U.S.A. 86 (7), 2336–2340.

Pati, S., Pelser, C.B., Dufraine, J., Bryant, J.L., Reitz Jr., M.S., Weichold, F.F., 2002. Antitumorigenic effects of HIV protease inhibitor ritonavir: inhibition of Kaposi sarcoma. Blood 99 (10), 3771–3779.

Pereira, L.A., Bentley, K., Peeters, A., Churchill, M.J., Deacon, N.J., 2000. A compilation of cellular transcription factor interactions with the HIV-1 LTR promoter. Nucleic Acids Res. 28 (3), 663–668.

Pierson, T., McArthur, J., Siliciano, R.F., 2000. Reservoirs for HIV-1: mechanisms for viral persistence in the presence of antiviral immune responses and antiretroviral therapy. Annu. Rev. Immunol. 18, 665–708.

Poli, G., Kinter, A.L., Fauci, A.S., 1994. Interleukin 1 induces expression of the human immunodeficiency virus alone and in synergy with interleukin 6 in chronically infected U1 cells: inhibition of inductive effects by the interleukin 1 receptor antagonist. Proc. Natl. Acad. Sci. U.S.A. 91 (1), 108–112.

Pomerantz, R.J., Horn, D.L., 2003. Twenty years of therapy for HIV-1 infection. Nat. Med. 9 (7), 867–873.

Siliciano, J.D., Kajdas, J., Finzi, D., Quinn, T.C., Chadwick, K., Margolick, J.B., Kovacs, C., Gange, S.J., Siliciano, R.F., 2003. Long-term follow-up studies confirm the stability of the latent reservoir for HIV-1 in resting $CD4^+$ T cells. Nat. Med. 9 (6), 727–728.

Takahashi, Y., Tanaka, Y., Yamashita, A., Koyanagi, Y., Nakamura, M., Yamamoto, N., 2001. OX40 stimulation by gp34/OX40 ligand enhances productive human immunodeficiency virus type 1 infection. J. Virol. 75 (15), 6748–6757.

Wong, J.K., Hezareh, M., Gunthard, H.F., Havlir, D.V., Ignacio, C.C., Spina, C.A., Richman, D.D., 1997. Recovery of replication-competent HIV despite prolonged suppression of plasma viremia. Science 278 (5341), 1291–1295.

JOURNAL OF VIROLOGY, Jan. 2008, p. 588–592
0022-538X/08/$08.00+0 doi:10.1128/JVI.01697-07

Vol. 82, No. 1

Heptad Repeat-Derived Peptides Block Protease-Mediated Direct Entry from the Cell Surface of Severe Acute Respiratory Syndrome Coronavirus but Not Entry via the Endosomal Pathway▽

Makoto Ujike,[1]† Hiroki Nishikawa,[2]† Akira Otaka,[3] Naoki Yamamoto,[4] Norio Yamamoto,[4] Masao Matsuoka,[5] Eiichi Kodama,[5] Nobutaka Fujii,[2,5]* and Fumihiro Taguchi[1]*

Department of Virology III, National Institute of Infectious Disease, Gakuen 4-7-1, Musashi-murayama, Tokyo 208-0011, Japan[1]; Graduate School of Pharmaceutical Sciences, Kyoto University, Sakyo-ku, Kyoto 606-8501, Japan[2]; Graduate School of Pharmaceutical Sciences, The University of Tokushima, Tokushima 770-8505, Japan[3]; Department of Molecular Virology, Tokyo Medical and Dental University, 1-5-45 Yushima, Bunkyo-ku, Tokyo 113-8519, Japan[4]; and Institute for Virus Research, Kyoto University, Sakyo-ku, Kyoto 606-8507, Japan[5]

Received 6 August 2007/Accepted 6 October 2007

The peptides derived from the heptad repeat (HRP) of severe acute respiratory syndrome coronavirus (SCoV) spike protein (sHRPs) are known to inhibit SCoV infection, yet their efficacies are fairly low. Recently our research showed that some proteases facilitated SCoV's direct entry from the cell surface, resulting in a more efficient infection than the previously known infection via endosomal entry. To compare the inhibitory effect of the sHRP in each pathway, we selected two sHRPs, which showed a strong inhibitory effect on the interaction of two heptad repeats in a rapid and virus-free in vitro assay system. We found that they efficiently inhibited SCoV infection of the protease-mediated cell surface pathway but had little effect on the endosomal pathway. This finding suggests that sHRPs may effectively prevent infection in the lungs, where SCoV infection could be enhanced by proteases produced in this organ. This is the first observation that HRP exhibits different effects on virus that takes the endosomal pathway and virus that enters directly from the cell surface.

Severe acute respiratory syndrome (SARS) coronavirus (SCoV) is a causative agent of life-threatening SARS (4, 7, 15, 31). Although the first outbreak of SARS was stamped out, an effective antiviral drug is still required for the treatment and prevention of possible future outbreaks. SCoV is an enveloped virus and enters cells via fusion between the cellular membrane and its envelope. SCoV membrane fusion is mediated by the spike (S) protein, which is classified as a class I fusion protein. One of the most important features of class I fusion proteins is the conserved heptad repeat regions (HR1 and HR2) which play an essential role in virus-cell fusion activities (3, 6, 10, 28). In the fusion process, HR1 forms an interior, trimeric coiled-coil structure to which HR2 binds in an antiparallel fashion, resulting in the formation of a six-helix bundle. This structure brings viral and cellular membranes into close proximity to facilitate membrane fusion. Synthetic short peptides derived from the HR (HRP) of class I fusion proteins have been shown to block the interaction of HR1-HR2 complexes, resulting in the inhibition of a number of viral infections, including those of retroviruses (11, 14, 21, 23, 32, 38, 39), paramyxoviruses (12, 16, 30, 36, 42–44), filovirus (37), and coronavirus (2). Similarly, HRP of SCoV S (sHRP) could also inhibit SCoV and human immunodeficiency virus (HIV)/SCoV-pseudotyped virus infection (1, 18, 24, 45). However, these inhibitory effects were significantly less than those of one of the most effective HRPs from HIV type 1 (HIV-1) (39) and even those from the same family, murine coronavirus mouse hepatitis virus (MHV) (2).

The major organs targeted by SCoV are the lungs and intestines, although the virus grows in a variety of tissues that express angiotensin-converting enzyme 2 (ACE2). Recently we and others showed that SCoV uses two distinct entry pathways depending on the presence of proteases (20, 33, 34). In the absence of proteases, SCoV enters the cell via an endosomal pathway (9, 26, 41), with the S protein activated for fusion by the cathepsin L protease, which is active only under acidic conditions in the endosome (8, 33). In contrast, in the presence of protease, SCoV virion S proteins attach to ACE2 on the host cell surface and are activated for fusion by proteases such as trypsin or elastase, which leads to envelope-plasma membrane fusion and direct entry from the cell surface (20, 33, 34). Infection via the cell surface is more than 100 times more efficient than infection via the endosomal pathway (20). These results suggested the possibility that the severe illnesses in the lung and intestine could be due to the enhancement of direct SCoV cell surface entry mediated by proteases produced in these organs (20).

Although previous studies have described the inhibitory effects of the sHRP on SCoV infection via the endosomal path-

* Corresponding author. Mailing address for F. Taguchi: Department of Virology III, National Institute of Infectious Disease, Gakuen 4-7-1, Musashi-murayama, Tokyo 208-0011, Japan. Phone: 81-42-561-0771, ext. 533. Fax: 81-42-567-5631. E-mail: ftaguchi@nih.go.jp. Mailing address for N. Fujii: Graduate School of Pharmaceutical Sciences, Kyoto University, Sakyo-ku, Kyoto 606-8501, Japan. Phone: 81-75-753-4511. Fax: 81-75-753-4570. E-mail: nfujii@pharm.kyoto-u.ac.jp.

† M.U. and H.N. contributed equally to this work.

▽ Published ahead of print on 17 October 2007.

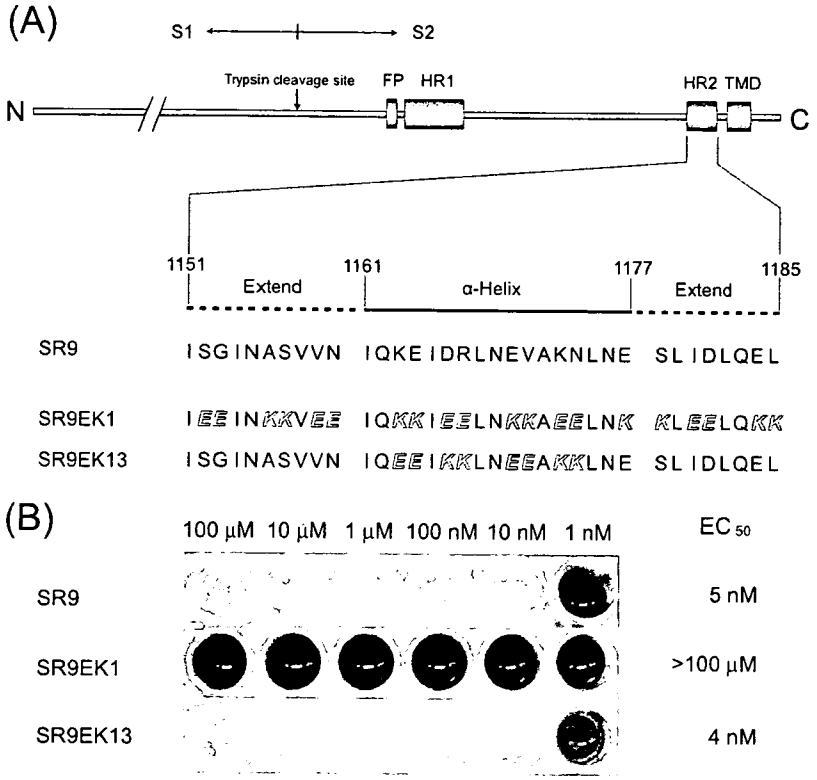

FIG. 1. (A) Schematic of SCoV S protein and sequences of native sHRP (SR9) and its EK substitution derivatives. The S protein contains two α-helical heptad repeats (HR1 and HR2), a putative fusion peptide (FP), a transmembrane domain (TMD), and a trypsin cleavage site (17). The expanded region shows the amino acid sequence of HR2 (SR9), which consists of two extended parts (1151 to 1160 and 1178 to 1185) and one α-helix part (1161 to 1177). Substituted EKs are shown with italic white letters. (B) In vitro binding inhibition assay of HRPs. GST-HR2-coated plates were incubated with MBP-HR1 in the presence of various concentrations (1 nM to 100 μM) of sHRP. Inhibitory potency of the peptide was assessed using the anti-MBP antibody-alkaline phosphatase conjugate and staining with 5-bromo-4-chloro-3-indolylphosphate.

way (1, 18, 24, 45), little is known about their effects on the protease-mediated cell surface pathway. Thus, in this study, we reevaluated the inhibitory effects of the sHRP on infection via the two distinct pathways of SCoV entry.

Recent studies of the X-ray crystal structure of the SCoV S HR1-HR2 complex have shown that the HR2 peptide consists of two extended regions and one α-helical region (35, 40). Since we have found that HRPs with replacement by the X-EE-XX-KK sequence in the HIV-1 HR2 region exhibited potent anti-HIV-1 activity (27), we chose to modify the α-helical region of HRP derived from SCoV S HR2 (sHRP) and also to prepare the control peptide SR9EK1 without sequence relatedness (Fig. 1A). To estimate these sHRPs, we established a rapid and virus-free in vitro novel assay system based on the inhibition of HR1-HR2 complex formation. Two fusion proteins (maltose binding protein [MBP]-HR1 [amino acid residues of the S protein, 892 to 964] and glutathione *S*-transferase [GST]-HR2 [1141 to 1192]) were expressed using *Escherichia coli* and purified using amylose resin (New England Biolabs) and glutathione Sepharose 4B (GE Healthcare, Bucks, United Kingdom), respectively. An enzyme-linked immunosorbent assay plate was coated with GST-HR2 dissolved in sodium carbonate buffer (pH 8.5), 3.6 μg/ml in concentration, by incubation at 4°C for 8 h. After bovine serum albumin blocking (1 mg/ml) at 4°C for 2.5 h, GST-HR2 on the plate was allowed to bind the MBP-HR1 protein (8.8 μg/ml) by incubation at 37°C for 1.5 h in the presence of various concentrations of sHRPs to be examined for inhibition activity. After the plate was washed, the inhibiting potency of the peptide was assessed by colorimetric analyses using the anti-MBP antibody-alkaline phosphatase conjugate (Sigma) with a 1:1,000 dilution with incubation at 4°C for 1 h and then staining with BluePhos microwell phosphatase (KPL). As shown in Fig. 1B, SR9 and SR9EK13 showed significant binding inhibition in a nanomolar range, whereas the control, SR9EK1, without sequence relatedness, had no inhibitory effect at a concentration of 100 μM.

We tested the inhibitory effects of SR9 and SR9EK13 on SCoV entry, since these sHRPs were found to have a strong binding inhibition activity, along with the control peptide SR9EK1. We examined their effects on both the endosomal and protease-mediated cell surface entry processes. Viral entry via the endosome was examined as described previously with a slight modification (20). In brief, VeroE6 cells were pretreated with each sHRP at 37°C for 30 min and then inoculated with SCoV (multiplicity of infection = 1.0) and incubated on ice for 30 min to allow viral attachment to ACE2 but not viral entry. After removal of unattached viruses, the cells were incubated at 37°C for 6 h. Viral entry was measured by quantifying the newly synthesized mRNA9 using real-time PCR (20). To evaluate entry via the cell surface, the cells were pretreated with 1

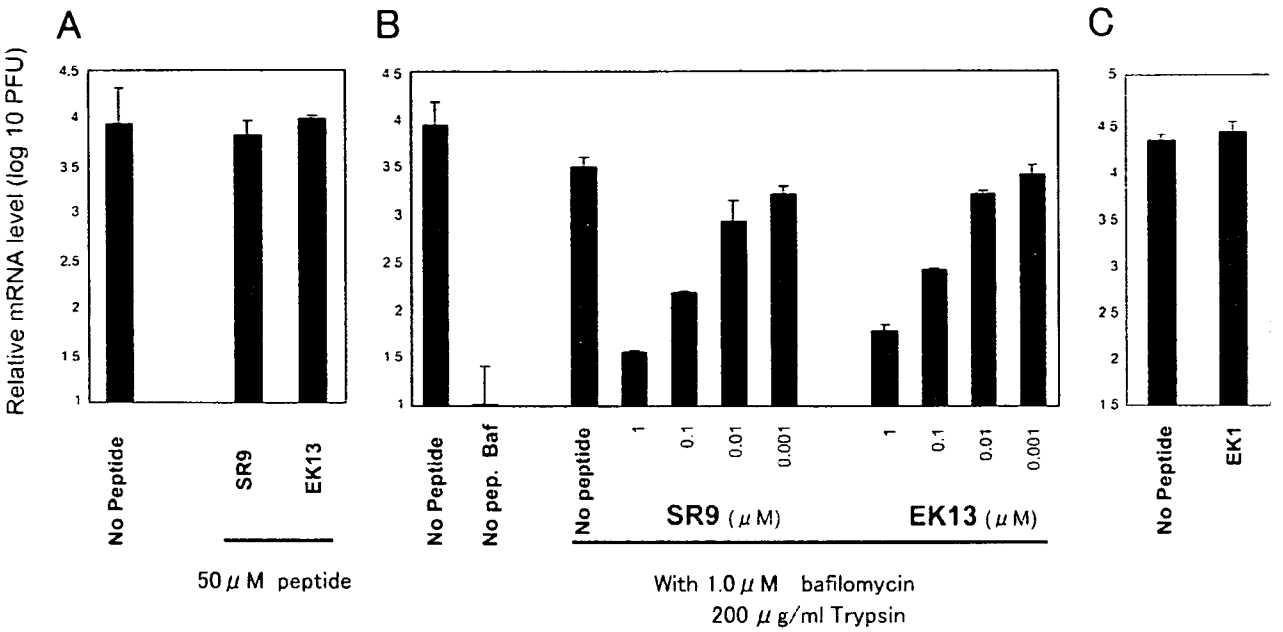

FIG. 2. Inhibitory effect of sHRPs on SCoV infections via the endosomal pathway (A) or protease-mediated cell-surface pathway (B). (A) VeroE6 cells were pretreated with 50 μM sHRPs at 37°C for 30 min, placed on ice for 10 min, and then inoculated with SCoV at a multiplicity of infection of 1.0 on ice for 30 min. After the removal of unbound virus, the cells were incubated in medium containing 50 μM sHRPs at 37°C for 6 h. (B) Cells pretreated with 1 μM Baf and sHRPs at the indicated concentrations were inoculated with SCoV as described above. After the removal of unbound virus, the cells were treated with 200 μg/ml L-1-tosylamide-2-phenylethyl chloromethyl ketone-treated trypsin at room temperature for 5 min and incubated at 37°C for 6 h. sHRP and Baf were present in the media in all steps at indicated concentrations. To measure amounts of viruses that entered cells, cells were infected with 10-fold-stepwise-diluted SARS-CoV from 10^6 to 10^2 PFU without Baf and trypsin and the amounts of mRNA9 were quantified by real-time PCR. Amounts of viral entry in this study were calculated from a calibration line obtained as described above and are shown as relative mRNA levels (20). (C) EK1 has no sequential similarity to sHRP and showed no inhibitory effect in vitro. Cells were treated with 1 μM EK1 as a control peptide, and other procedures were performed as described for panel B.

μM bafilomycin (Baf), which blocks SCoV endosomal entry, at 37°C for 30 min before SCoV inoculation. After removal of unattached viruses, the cells were treated with trypsin (0.2 mg/ml) for 5 min at room temperature and viral entry was measured as described above. Each sHRP and/or Baf was present in the media in all steps at various concentrations. In the absence of proteases, these sHRPs showed no measurable inhibitory effect on SCoV endosomal infection even at concentrations as high as 50 μM, despite showing a potent inhibitory effect in vitro (Fig. 2A). This lack of inhibition is consistent with previous observations that the same or homologous-sequence sHRPs had no inhibitory effect on SCoV infection at high concentrations of 10 μM (45) or 50 μM (1), respectively. In contrast, when SCoV was allowed to enter cells via the cell surface by treatment with protease and Baf, these sHRPs showed a strong inhibitory effect on SCoV infection in a dose-dependent manner (Fig. 2B). At a concentration of 0.1 μM, the SR9 sHRP reduced newly synthesized mRNA9 levels by about 10-fold, while an sHRP concentration of 1 μM saw a 50-fold decrease. The control sHRP, SR9EK1, did not inhibit SCoV cell-surface-mediated infection even at the concentration of 1 μM, indicating that the inhibition is peptide sequence specific (Fig. 2C). We finally evaluated the inhibitory effect of sHRPs in the presence of trypsin but without Baf treatment. These conditions may resemble the situation of patients with severe SARS, in which some proteases were produced in the infected lung and intestinal tissue. Under these conditions, these sHRPs also showed a potent inhibitory effect on SCoV infection (Fig. 3).

The present study indicates that our sHRPs fail to inhibit endosome-mediated SCoV infection. This finding is consistent with those of previous studies indicating that sHRPs have a low inhibitory effect on endosomal infection of native SCoV. The reported 50% effective dose (EC_{50}) was 3.68 to 19.0 μM (1, 18, 45). However, our results suggest that sHRPs, which showed no measurable inhibitory effect on SCoV endosomal infection, have a very strong inhibitory effect on protease-mediated cell surface SCoV infection; the EC_{50} was less than 100 nM (Fig. 2B and 3). Cell surface infection of SCoV is anticipated to occur in the lungs of SARS patients, since various types of inflammatory cells infiltrate the lung of the patients (25), and thus elastase, a protease produced in lung inflammation (13) and shown to enhance SCoV infection in cultured cells (20), could enhance SCoV infection in the lung by facilitating the infection from cell surface. Inhibitory effects of sHRPs on cell surface infection may help prevent severe damage by SCoV infection in the major target organ. Thus, the sHRPs shown in this study would be effective anti-SARS therapeutic drugs.

A few possibilities are conceivable for the explanation of an inefficient inhibitory effect of sHRPs in infection via the endosomal pathway. One is the failure of sHRPs to be trafficked to the endosome vehicles from culture medium. Thus, their concentration in the endosome is not sufficient to prevent SCoV infection. Alternatively, sHRPs may be sufficiently transported

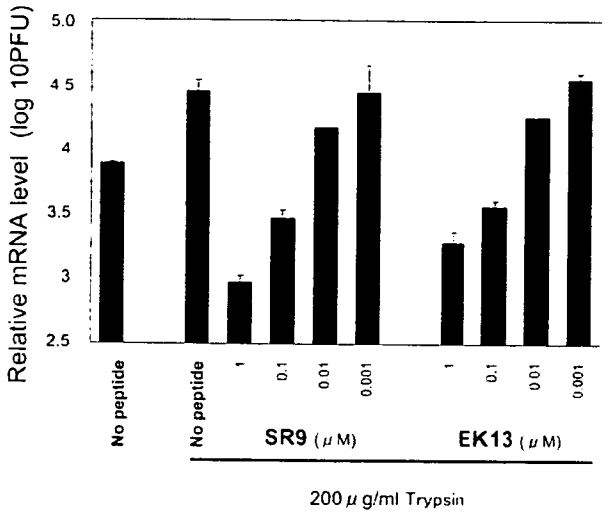

FIG. 3. Effective inhibition by HRPs of SCoV infection in the presence of exogenous trypsin. VeroE6 cells pretreated with sHRPs at the indicated concentrations were inoculated with SCoV as described in the legend to Fig. 2. After the removal of unbound virus, the cells were treated with 200 μg/ml L-1-tosylamide-2-phenylethyl chloromethyl ketone-treated trypsin at room temperature for 5 min and incubated at 37°C for 6 h. sHRPs were present in the media in all steps at the indicated concentrations. The relative viral mRNA9 was measured quantitatively by real-time PCR as described in the legend to Fig. 2. In this assay, cells were not treated with Baf throughout the experiment.

to the endosome but are inactivated by the low-pH environment or are degraded or digested with proteases present in the endosome. Another possibility is that the conformation of the cleaved S protein in the acidic environment of the endosome is different from that in a neutral pH and the sHRP fails to bind to the S protein in the former environment even if six-helix bundles with intramolecular HR2 are formed under both conditions. We are currently studying whether the inefficient inhibition of virus entry into cells could be attributed to one of those possibilities, or even another.

Interestingly, the EC_{50} (approximately 680 μM) of HRP of Ebola virus (37), which is thought to enter cells via an endosomal pathway, is remarkably higher than those of other viruses which enter cells directly from the cell surface. The inhibition with HRP of influenza virus infection, which also uses an endosomal pathway, has not yet been reported, even though its hemagglutinin protein is the prototype class I fusion protein and its cell entry mechanism has been extensively studied. In contrast, HRP of avian leucosis sarcoma virus, which uses the endosomal pathway, was reported to inhibit the infection fairly efficiently (EC_{50} = 25 to 170 nM) (5, 23). The inhibition, however, was executed during the conformational rearrangement of the envelope protein that occurs on the cell surface following attachment to the receptor and facilitates the exposure of HRs but not later than the transport into the endosome, where the avian leucosis sarcoma virus genome enters the cytoplasm by its envelope and endosomal membrane fusion in a low-pH environment (19, 22, 23). These observations together with those of the present study and others (1, 18, 24, 45) suggest that the HRPs have very low or little inhibitory effect in the endosome. If the above assumption is correct and the HRPs were designed to be efficiently transferred into the endosome and to be stable in the environment, they may be new antiviral candidates against those viruses that take the endosomal entry pathway, such as influenza virus, Ebola virus, and SCoV. Thus, detailed molecular studies on SCoV and the sHRP will provide a good model for the development and evaluation of such endosome-philic antiviral peptide inhibitors.

Recent studies have reported that the low inhibitory effect of the SCoV sHRP compared to that of the MHV HRP could be attributed to the weaker interaction of the SCoV S HR1-HR2 complex versus that of MHV S (1, 2). However, SCoV infection was efficiently blocked by sHRP under certain conditions, as revealed in this study; the concentration of sHRPs needed to inhibit SCoV infection is even lower than that required for MHV inhibition (1, 2). The apparent difference between MHV and SCoV infection is the pathway used to enter cells; the former enters directly from the cell surface, whereas the latter takes an endosomal pathway. Both MHV and SCoV infections were efficiently blocked when these viruses utilized the cell surface pathway for entry. These observations suggest that the lower HRP inhibitory effect on SCoV could be due to different entry pathways between SCoV and MHV rather than the weaker interaction of the HRP and SCoV S. To further explore this possibility, studies are ongoing to determine the effect of MHV sHRPs on infection by MHV-2, which, like SCoV, utilizes an endosomal infection pathway (29).

We thank Miyuki Kawase for her excellent technical assistance and Shutoku Matsuyama for his valuable discussions.

This work was financially supported by grants from the Ministry of Education, Culture, Sports, Science and Technology.

REFERENCES

1. **Bosch, B. J., B. E. Martina, R. Van Der Zee, J. Lepault, B. J. Haijema, C. Versluis, A. J. Heck, R. De Groot, A. D. Osterhaus, and P. J. Rottier.** 2004. Severe acute respiratory syndrome coronavirus (SARS-CoV) infection inhibition using spike protein heptad repeat-derived peptides. Proc. Natl. Acad. Sci. USA **101**:8455–8460.
2. **Bosch, B. J., R. van der Zee, C. A. de Haan, and P. J. Rottier.** 2003. The coronavirus spike protein is a class I virus fusion protein: structural and functional characterization of the fusion core complex. J. Virol. **77**:8801–8811.
3. **Chan, W. E., C. K. Chuang, S. H. Yeh, M. S. Chang, and S. S. Chen.** 2006. Functional characterization of heptad repeat 1 and 2 mutants of the spike protein of severe acute respiratory syndrome coronavirus. J. Virol. **80**:3225–3237.
4. **Drosten, C., S. Gunther, W. Preiser, S. van der Werf, H. R. Brodt, S. Becker, H. Rabenau, M. Panning, L. Kolesnikova, R. A. Fouchier, A. Berger, A. M. Burguiere, J. Cinatl, M. Eickmann, N. Escriou, K. Grywna, S. Kramme, J. C. Manuguerra, S. Muller, V. Rickerts, M. Sturmer, S. Vieth, H. D. Klenk, A. D. Osterhaus, H. Schmitz, and H. W. Doerr.** 2003. Identification of a novel coronavirus in patients with severe acute respiratory syndrome. N. Engl. J. Med. **348**:1967–1976.
5. **Earp, L. J., S. E. Delos, R. C. Netter, P. Bates, and J. M. White.** 2003. The avian retrovirus avian sarcoma/leukosis virus subtype A reaches the lipid mixing stage of fusion at neutral pH. J. Virol. **67**:3058–3066.
6. **Follis, K. E., J. York, and J. H. Nunberg.** 2005. Serine-scanning mutagenesis studies of the C-terminal heptad repeats in the SARS coronavirus S glycoprotein highlight the important role of the short helical region. Virology **341**:122–129.
7. **Fouchier, R. A., T. Kuiken, M. Schutten, G. van Amerongen, G. J. van Doornum, B. G. van den Hoogen, M. Peiris, W. Lim, K. Stohr, and A. D. Osterhaus.** 2003. Aetiology: Koch's postulates fulfilled for SARS virus. Nature **423**:240.
8. **Huang, I. C., B. J. Bosch, F. Li, W. Li, K. H. Lee, S. Ghiran, N. Vasilieva, T. S. Dermody, S. C. Harrison, P. R. Dormitzer, M. Farzan, P. J. Rottier, and H. Choe.** 2006. SARS coronavirus, but not human coronavirus NL63, utilizes cathepsin L to infect ACE2-expressing cells. J. Biol. Chem. **281**:3198–3203.
9. **Inoue, Y., N. Tanaka, Y. Tanaka, S. Inoue, K. Morita, M. Zhuang, T. Hattori, and K. Sugamura.** 2007. Clathrin-dependent entry of severe acute respira-

tory syndrome coronavirus into target cells expressing ACE2 with the cytoplasmic tail deleted. J. Virol. 81:8722–8729.
10. Jahn, R., T. Lang, and T. C. Sudhof. 2003. Membrane fusion. Cell 112:519–533.
11. Jiang, S., K. Lin, N. Strick, and A. R. Neurath. 1993. HIV-1 inhibition by a peptide. Nature 365:113.
12. Joshi, S. B., R. E. Dutch, and R. A. Lamb. 1998. A core trimer of the paramyxovirus fusion protein: parallels to influenza virus hemagglutinin and HIV-1 gp41. Virology 248:20–34.
13. Kawabata, K., T. Hagio, and S. Matsuoka. 2002. The role of neutrophil elastase in acute lung injury. Eur. J. Pharmacol. 451:1–10.
14. Kilby, J. M., S. Hopkins, T. M. Venetta, B. DiMassimo, G. A. Cloud, J. Y. Lee, L. Alldredge, E. Hunter, D. Lambert, D. Bolognesi, T. Matthews, M. R. Johnson, M. A. Nowak, G. M. Shaw, and M. S. Saag. 1998. Potent suppression of HIV-1 replication in humans by T-20, a peptide inhibitor of gp41-mediated virus entry. Nat. Med. 4:1302–1307.
15. Ksiazek, T. G., D. Erdman, C. S. Goldsmith, S. R. Zaki, T. Peret, S. Emery, S. Tong, C. Urbani, J. A. Comer, W. Lim, P. E. Rollin, S. F. Dowell, A. E. Ling, C. D. Humphrey, W. J. Shieh, J. Guarner, C. D. Paddock, P. Rota, B. Fields, J. DeRisi, J. Y. Yang, N. Cox, J. M. Hughes, J. W. LeDuc, W. J. Bellini, and L. J. Anderson. 2003. A novel coronavirus associated with severe acute respiratory syndrome. N. Engl. J. Med. 348:1953–1966.
16. Lambert, D. M., S. Barney, A. L. Lambert, K. Guthrie, R. Medinas, D. E. Davis, T. Bucy, J. Erickson, G. Merutka, and S. R. Petteway, Jr. 1996. Peptides from conserved regions of paramyxovirus fusion (F) proteins are potent inhibitors of viral fusion. Proc. Natl. Acad. Sci. USA 93:2186–2191.
17. Li, F., M. Berardi, W. Li, M. Farzan, P. R. Dormitzer, and S. C. Harrison. 2006. Conformational states of the severe acute respiratory syndrome coronavirus spike protein ectodomain. J. Virol. 80:6794–6800.
18. Liu, S., G. Xiao, Y. Chen, Y. He, J. Niu, C. R. Escalante, H. Xiong, J. Farmar, A. K. Debnath, P. Tien, and S. Jiang. 2004. Interaction between heptad repeat 1 and 2 regions in spike protein of SARS-associated coronavirus: implications for virus fusogenic mechanism and identification of fusion inhibitors. Lancet 363:938–947.
19. Matsuyama, S., S. E. Delos, and J. M. White. 2004. Sequential roles of receptor binding and low pH in forming prehairpin and hairpin conformations of a retroviral envelope glycoprotein. J. Virol. 78:8201–8209.
20. Matsuyama, S., M. Ujike, S. Morikawa, M. Tashiro, and F. Taguchi. 2005. Protease-mediated enhancement of severe acute respiratory syndrome coronavirus infection. Proc. Natl. Acad. Sci. USA 102:12543–12547.
21. Medinas, R. J., D. M. Lambert, and W. A. Tompkins. 2002. C-Terminal gp40 peptide analogs inhibit feline immunodeficiency virus: cell fusion and virus spread. J. Virol. 76:9079–9086.
22. Melikyan, G. B., R. J. Barnard, R. M. Markosyan, J. A. Young, and F. S. Cohen. 2004. Low pH is required for avian sarcoma and leukosis virus Env-induced hemifusion and fusion pore formation but not for pore growth. J. Virol. 78:3753–3762.
23. Netter, R. C., S. M. Amberg, J. W. Balliet, M. J. Biscone, A. Vermeulen, L. J. Earp, J. M. White, and P. Bates. 2004. Heptad repeat 2-based peptides inhibit avian sarcoma and leukosis virus subgroup a infection and identify a fusion intermediate. J. Virol. 78:13430–13439.
24. Ni, L., J. Zhu, J. Zhang, M. Yan, G. F. Gao, and P. Tien. 2005. Design of recombinant protein-based SARS-CoV entry inhibitors targeting the heptad-repeat regions of the spike protein S2 domain. Biochem. Biophys. Res. Commun. 330:39–45.
25. Nicholls, J. M., L. L. Poon, K. C. Lee, W. F. Ng, S. T. Lai, C. Y. Leung, C. M. Chu, P. K. Hui, K. L. Mak, W. Lim, K. W. Yan, K. H. Chan, N. C. Tsang, Y. Guan, K. Y. Yuen, and J. S. Peiris. 2003. Lung pathology of fatal severe acute respiratory syndrome. Lancet 361:1773–1778.
26. Nie, Y., P. Wang, X. Shi, G. Wang, J. Chen, A. Zheng, W. Wang, Z. Wang, X. Qu, M. Luo, L. Tan, X. Song, X. Yin, J. Chen, M. Ding, and H. Deng. 2004. Highly infectious SARS-CoV pseudotyped virus reveals the cell tropism and its correlation with receptor expression. Biochem. Biophys. Res. Commun. 321:994–1000.
27. Otaka, A., M. Nakamura, D. Nameki, E. Kodama, S. Uchiyama, S. Nakamura, H. Nakano, H. Tamamura, Y. Kobayashi, M. Matsuoka, and N. Fujii. 2002. Remodeling of gp41-C34 peptide leads to highly effective inhibitors of the fusion of HIV-1 with target cells. Angew. Chem. Int. Ed. Engl. 41:2937–2940.
28. Petit, C. M., J. M. Melancon, V. N. Chouljenko, R. Colgrove, M. Farzan, D. M. Knipe, and K. G. Kousoulas. 2005. Genetic analysis of the SARS-coronavirus spike glycoprotein functional domains involved in cell-surface expression and cell-to-cell fusion. Virology 341:215–230.
29. Qiu, Z., S. T. Hingley, G. Simmons, C. Yu, J. Das Sarma, P. Bates, and S. R. Weiss. 2006. Endosomal proteolysis by cathepsins is necessary for murine coronavirus mouse hepatitis virus type 2 spike-mediated entry. J. Virol. 80:5768–5776.
30. Rapaport, D., M. Ovadia, and Y. Shai. 1995. A synthetic peptide corresponding to a conserved heptad repeat domain is a potent inhibitor of Sendai virus-cell fusion: an emerging similarity with functional domains of other viruses. EMBO J. 14:5524–5531.
31. Rota, P. A., M. S. Oberste, S. S. Monroe, W. A. Nix, R. Campagnoli, J. P. Icenogle, S. Penaranda, B. Bankamp, K. Maher, M. H. Chen, S. Tong, A. Tamin, L. Lowe, M. Frace, J. L. DeRisi, Q. Chen, D. Wang, D. D. Erdman, T. C. Peret, C. Burns, T. G. Ksiazek, P. E. Rollin, A. Sanchez, S. Liffick, B. Holloway, J. Limor, K. McCaustland, M. Olsen-Rasmussen, R. Fouchier, S. Gunther, A. D. Osterhaus, C. Drosten, M. A. Pallansch, L. J. Anderson, and W. J. Bellini. 2003. Characterization of a novel coronavirus associated with severe acute respiratory syndrome. Science 300:1394–1399.
32. Sagara, Y., Y. Inoue, H. Shiraki, A. Jinno, H. Hoshino, and Y. Maeda. 1996. Identification and mapping of functional domains on human T-cell lymphotropic virus type 1 envelope proteins by using synthetic peptides. J. Virol. 70:1564–1569.
33. Simmons, G., D. N. Gosalia, A. J. Rennekamp, J. D. Reeves, S. L. Diamond, and P. Bates. 2005. Inhibitors of cathepsin L prevent severe acute respiratory syndrome coronavirus entry. Proc. Natl. Acad. Sci. USA 102:11876–11881.
34. Simmons, G., J. D. Reeves, A. J. Rennekamp, S. M. Amberg, A. J. Piefer, and P. Bates. 2004. Characterization of severe acute respiratory syndrome-associated coronavirus (SARS-CoV) spike glycoprotein-mediated viral entry. Proc. Natl. Acad. Sci. USA 101:4240–4245.
35. Supekar, V. M., C. Bruckmann, P. Ingallinella, E. Bianchi, A. Pessi, and A. Carfi. 2004. Structure of a proteolytically resistant core from the severe acute respiratory syndrome coronavirus S2 fusion protein. Proc. Natl. Acad. Sci. USA 101:17958–17963.
36. Wang, E., X. Sun, Y. Qian, L. Zhao, P. Tien, and G. F. Gao. 2003. Both heptad repeats of human respiratory syncytial virus fusion protein are potent inhibitors of viral fusion. Biochem. Biophys. Res. Commun. 302:469–475.
37. Watanabe, S., A. Takada, T. Watanabe, H. Ito, H. Kida, and Y. Kawaoka. 2000. Functional importance of the coiled-coil of the Ebola virus glycoprotein. J. Virol. 74:10194–10201.
38. Wild, C., T. Oas, C. McDanal, D. Bolognesi, and T. Matthews. 1992. A synthetic peptide inhibitor of human immunodeficiency virus replication: correlation between solution structure and viral inhibition. Proc. Natl. Acad. Sci. USA 89:10537–10541.
39. Wild, C. T., D. C. Shugars, T. K. Greenwell, C. B. McDanal, and T. J. Matthews. 1994. Peptides corresponding to a predictive alpha-helical domain of human immunodeficiency virus type 1 gp41 are potent inhibitors of virus infection. Proc. Natl. Acad. Sci. USA 91:9770–9774.
40. Xu, Y., Z. Lou, Y. Liu, H. Pang, P. Tien, G. F. Gao, and Z. Rao. 2004. Crystal structure of severe acute respiratory syndrome coronavirus spike protein fusion core. J. Biol. Chem. 279:49414–49419.
41. Yang, Z. Y., Y. Huang, L. Ganesh, K. Leung, W. P. Kong, O. Schwartz, K. Subbarao, and G. J. Nabel. 2004. pH-dependent entry of severe acute respiratory syndrome coronavirus is mediated by the spike glycoprotein and enhanced by dendritic cell transfer through DC-SIGN. J. Virol. 78:5642–5650.
42. Yao, Q., and R. W. Compans. 1996. Peptides corresponding to the heptad repeat sequence of human parainfluenza virus fusion protein are potent inhibitors of virus infection. Virology 223:103–112.
43. Young, J. K., D. Li, M. C. Abramowitz, and T. G. Morrison. 1999. Interaction of peptides with sequences from the Newcastle disease virus fusion protein heptad repeat regions. J. Virol. 73:5945–5956.
44. Yu, M., E. Wang, Y. Liu, D. Cao, N. Jin, C. W. Zhang, M. Bartlam, Z. Rao, P. Tien, and G. F. Gao. 2002. Six-helix bundle assembly and characterization of heptad repeat regions from the F protein of Newcastle disease virus. J. Gen. Virol. 83:623–629.
45. Yuan, K., L. Yi, J. Chen, X. Qu, T. Qing, X. Rao, P. Jiang, J. Hu, Z. Xiong, Y. Nie, X. Shi, W. Wang, C. Ling, X. Yin, K. Fan, L. Lai, M. Ding, and H. Deng. 2004. Suppression of SARS-CoV entry by peptides corresponding to heptad regions on spike glycoprotein. Biochem. Biophys. Res. Commun. 319:746–752.